

Capacitor Voltage Estimation Scheme with Reduced Number of Sensors for Modular Multilevel Converters

Osama SH. Mohamed Abushafa, Shady M. Gadoue, Mohamed S. A. Dahidah, *Senior Member, IEEE*, David J. Atkinson, *Member, IEEE* and Petros Missailidis.

Abstract—This paper presents a new method to measure the voltage across the submodule (SM) capacitors in a modular multilevel converter (MMC). The proposed technique requires only one voltage sensor per arm. This reduces the number of sensors required compared to conventional sensor-based methods. Therefore, the cost and complexity of the system are reduced, which in turn improves the converter's overall reliability. The proposed method employs an exponentially weighted recursive least square (ERLS) algorithm to estimate the SM capacitor voltages through the measured total arm voltage and the switching patterns of each SM. There is thus no need for extra sensors to measure these control signals as they are directly provided from the controller. The robustness of the proposed method is confirmed via introducing deviations for the capacitance values, dynamic load changes, DC voltage change and start-up transient condition. Simulation and experimentally validated results based on a single-phase MMC show the effectiveness of the proposed method in both, steady-state and dynamic operations.

Index Terms-- Modular multilevel converter (MMC); reduced number of sensors; pulse width modulation (PWM); recursive least square (RLS); voltage balancing control algorithm.

I. INTRODUCTION

The modular multilevel converter (MMC) was first introduced in 2003 by Lesnicar and Marquardt [1]. Since that time, the MMC has become one of the most attractive topologies for medium- and high-voltage applications due to its distinctive features when compared with the conventional multilevel converters.

Manuscript received September 07, 2017; revised December 08, 2017; accepted January 04, 2018. This work was supported by Libyan Ministry of Higher Education and Scientific Research and Scholar Program of Zawia and Sabratha Universities. Osama SH. Mohamed Abushafa is with Turbo Power Systems LTD company and also with the Department of Electrical Engineering, Faculty of Engineering, Sabratha University, Libya (e-mail: abushafa@turbopowersystems.com). Mohamed S. A. Dahidah, Dave G. Atkinson and Petros Missailidis are with the School of Engineering, Newcastle University, Newcastle upon Tyne, NE1 7RU, UK. S. M. Gadoue is with the School of Engineering and Applied Science, Aston University, Birmingham, B4 7ET, U.K., and also with the Department of Electrical Engineering, Faculty of Engineering, Alexandria University, Alexandria 21544, Egypt.

These features include: low harmonic distortion, flexibility and expandability in converter structure, and low switching losses [2-8]. These advantages have made the MMC a promising candidate for various applications such as battery storage systems, variable speed drives, flexible AC transmission systems (FACTS) [2, 9], and high-voltage direct current systems (HVDC) [3, 10-13].

Over the last few years, the popularity of the MMC has grown rapidly. However, extensive research has been carried out to address various issues associated with the control and the operation of MMC. As the converter usually consists of a large number of series cascaded submodules (SMs), the converter's reliability becomes an important challenge [14]. The voltage-balancing of the SM capacitors within the same arm with an acceptable voltage ripple is another serious concern for the operation of such a converter. This issue has been widely investigated in recent literature [15-21]; however, voltage and current sensors are always required to achieve voltage-balancing. Recent HVDC applications based on the MMC have involved the use of hundreds of SMs per phase [3]. In such applications, enormous numbers of voltage sensors are usually required to guarantee the voltage-balancing of the SM's capacitors. This will not only influence the converter cost, but also the reliability and complexity especially when a converter with high number of levels is considered.

There have been several attempts in recent years aiming to minimise the number of sensors required. For example, promises have been experimentally achieved with fewer current sensors [22-24], but in such studies the number of voltage sensors employed was not discussed. An open-loop approach has also been proposed with a fixed pulse pattern [25]. However, as the proposed topology does not use any form of feedback control, the well-known drawbacks of open-loop control techniques can significantly compromise the performance of the converter. Estimation techniques based on online observers have been recently proposed [26-28]. For instance a sliding mode observer is proposed in [26], where only monitoring the total input voltage and arm current of the converter are required. On the other hand, some practical issues such as the effect of deviation of SM capacitance have

not been considered. An improvement to the latter research [26] which involves the estimation of the capacitance value as well as the capacitor voltage of the SM capacitors was subsequently proposed in [27]. Although this improves the robustness of the system against capacitance uncertainty, however, the effect of the variation associated with the arm inductor value was not considered in the observer design. On the other hand, authors in the same study [27] have proved that the converter can perform well with up to +10% of the nominal arm inductor value. In more recent research [29], the voltage-balancing of a seven-level MMC has been achieved with fewer voltage sensors, where for each arm the minimum number of voltage sensor required is two. Although, this method has made an important achievement in reducing the number of voltage sensors; however an advanced voltage-balancing algorithm has to be applied to the system where activating and deactivating several SMs instantaneously may lead to instability. Consequently, voltage-balancing algorithm in that study [29] must provide one measurement per sample.

This paper proposes a new voltage estimation method aiming to reduce the number of the voltage sensors in the MMC, where only one voltage sensor per arm is required to ensure voltage-balancing of the converter. This sensor is connected to the total arm output voltage of the SMs. In the proposed technique, an exponentially weighted recursive least square (ERLS) algorithm is employed, for the first time in MMC applications, to estimate the voltage across each SM capacitor. Compared to conventional least square-based techniques, the proposed ERLS algorithm can reduce the computational complexity and is more suitable for time-varying dynamic systems. The proposed technique requires only the measured total arm voltage and the switching states of the SMs. These switching state values are obtained from the digital signal processor (DSP) controller and hence no extra sensors are required. Using this algorithm, there is no need to apply an advanced voltage-balancing method as any conventional scheme can be applied. The proposed method is independent of the voltage-balancing technique used, and for simplicity the conventional sorting algorithm was used in this paper. Moreover, due to the fact that measurement of voltages across arm inductors is not required in the algorithm design, this makes the proposed method independent of the variation of the arm inductor value. Tests have been carried out to evaluate the proposed method in terms of capacitance deviations, dynamic load change, DC voltage change and start-up transient condition. The proposed technique not only decreases the cost and complexity of the converter, but it can also be used for predictive control and fault detection algorithms with the aim of improving the general performance of the MMC. It worth noting that the proposed scheme can be

also applied for other multilevel converters, such as flying capacitor converter (FCC) and cascaded H-bridge converter (CHC).

The rest of the paper is organised as follows: Section II presents the principle of operation and the structure of MMC. Section III describes in detail the proposed estimation technique. Section IV and V present and discuss extensive simulation and experimentally validated results, respectively. Finally, the main conclusions of this study are summarized in Section VI.

II. PRINCIPLES OF OPERATION AND STRUCTURE OF MMCS

For the sake of simplicity, only a single phase (i.e. one leg) MMC is considered and analyzed in this study to proof the concept of the proposed method; however, the technique can be easily applied to three-phase MMCs. Fig. 1 (a) shows a single-phase circuit configuration of the MMC. For this configuration, the converter consists of two arms; each of them has a series connection of cascaded SMs and an arm inductor (L_s). In most cases the configuration of these SMs is either half-bridge or full-bridge configurations as illustrated in Fig. 1 (b) and (c). However, different arrangements can be also found in the literature, such as three-level flying capacitor (FC) or three-level neutral point clamped (NPC) [2]. The application attached to the converter will define which arrangement fits better for the system [9].

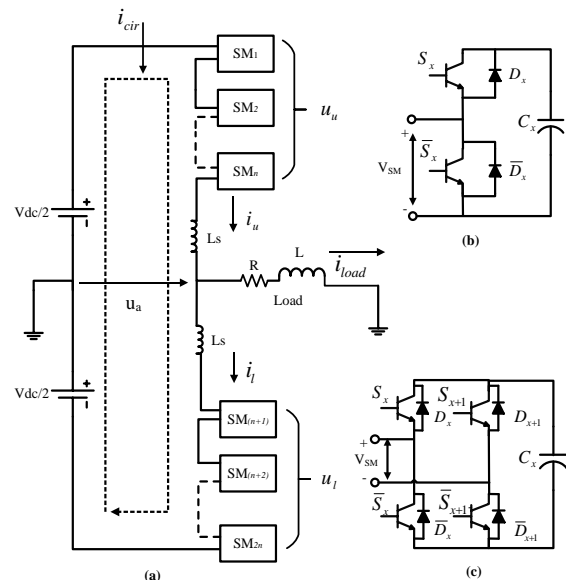


Fig. 1. Block diagram of MMC. (a) Single-phase (one-leg) Block diagram. (b) Half-bridge SM configuration. (c) Full-bridge SM configuration.

For the half-bridge configuration, switches S_x and \bar{S}_x decide the state of the SM. If S_x is **ON**, the output voltage of the SM (V_{SM}) will be equal to the voltage across the capacitor C_x (V_{Cx}), where $x = 1, 2, \dots, 2n$, and n is the number of SMs per arm. However, \bar{S}_x must be **OFF** while S_x is **ON**, this known as an **ON**

state. On the other hand, if S_x is **OFF** and \bar{S}_x is **ON** the output of the SM is equal to zero, i.e. the SM is

bypassed [19]. Table I summaries the relationship between the SM switches (S_x and \bar{S}_x) and the SM state.

TABLE I
STATES OF THE SM AND SWITCHING SIGNALS

State of the SM	S_x	\bar{S}_x	V_{SM}
ON	ON	OFF	V_{cx}
OFF	OFF	ON	0

The relationship between the upper current (i_u), lower current (i_l), circulating current (i_{cir}) and load current (i_{load}) can be defined as follows [18]:

$$i_u = i_{cir} + \frac{i_{load}}{2} \quad (1)$$

$$i_l = i_{cir} - \frac{i_{load}}{2} \quad (2)$$

In Fig. 1(a), the output voltage of the converter (u_a) can be expressed as follows [23]:

$$u_a = \frac{u_l - u_u}{2} - \frac{L_s}{2} \frac{di_{load}}{dt} \quad (3)$$

where u_u is the total output voltage of the upper cascaded SMs (from 1 to n) and u_l is the total output voltage of the lower cascaded SMs (from $(n+1)$ to $2n$).

III. PROPOSED ESTIMATION TECHNIQUE FOR MMCs

A. Modelling and System Configuration of the SMs

In the current study, only the half-bridge configuration is examined. However, the proposed estimation technique can be equally applied for full-bridge configuration as well; bearing in mind the unique relationship between switching signals and SM states.

In the proposed scheme, only one voltage sensor is required for each arm as illustrated in Fig. 2. The upper sensor is connected at the output of the series-cascaded SMs, where the connection is performed between the top terminal point of the first SM (SM_1) and the bottom terminal point of the last SM (SM_n) within this arm. Similar to the upper arm, the sensor for the lower arm is connected between $SM_{(n+1)}$ and SM_{2n} .

This arrangement makes the method independent of parameter variation associated with the arm inductor value. For an N -level converter; where $N = (1 + n)$, the total voltage SMs of the upper and lower arms in Fig. 2 can be modelled respectively as follows:

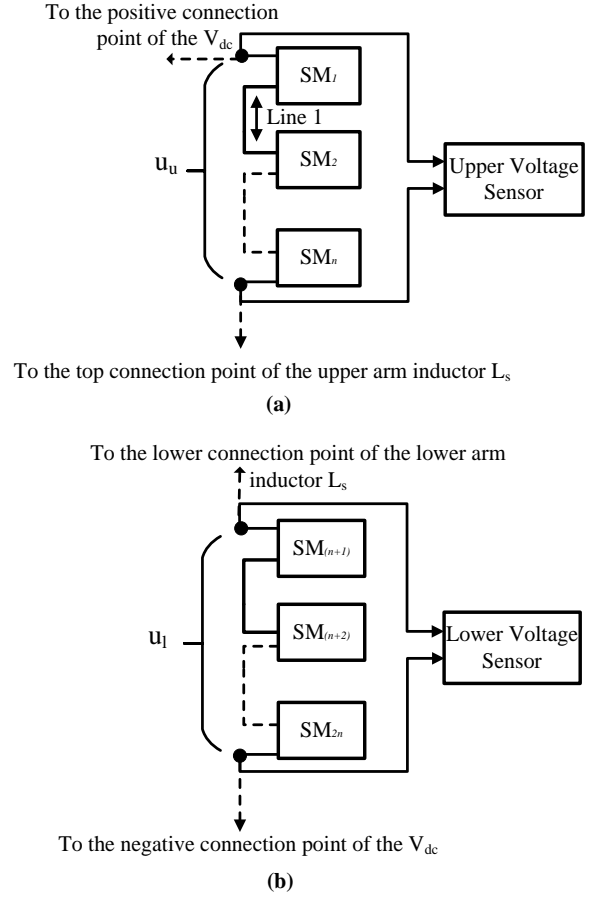


Fig. 2. Connection arrangement of the proposed estimation technique for the MMC. (a) Upper voltage sensor arrangement. (b) Lower voltage sensor arrangement.

$$\begin{aligned} \mathbf{u}_u(t_0) &= S_1(t_0) \mathbf{V}_{c1}(t_0) + \dots \\ &\quad + S_n(t_0) \mathbf{V}_{cn}(t_0) \\ \mathbf{u}_u(t_1) &= S_1(t_1) \mathbf{V}_{c1}(t_1) + \dots \\ &\quad + S_n(t_1) \mathbf{V}_{cn}(t_1) \\ \vdots &= \vdots + \dots + \vdots \\ \mathbf{u}_u(t_j) &= S_1(t_j) \mathbf{V}_{c1}(t_j) + \dots \\ &\quad + S_n(t_j) \mathbf{V}_{cn}(t_j) \end{aligned} \quad (4)$$

$$\begin{aligned} \mathbf{u}_l(t_0) &= S_{n+1}(t_0) \mathbf{V}_{c(n+1)}(t_0) + \dots \\ &\quad + S_{2n}(t_0) \mathbf{V}_{c2n}(t_0) \\ \mathbf{u}_l(t_1) &= S_{n+1}(t_1) \mathbf{V}_{c(n+1)}(t_1) + \dots \\ &\quad + S_{2n}(t_1) \mathbf{V}_{c2n}(t_1) \\ \vdots &= \vdots + \dots + \vdots \\ \mathbf{u}_l(t_j) &= S_{n+1}(t_j) \mathbf{V}_{c(n+1)}(t_j) + \dots \\ &\quad + S_{2n}(t_j) \mathbf{V}_{c2n}(t_j) \end{aligned} \quad (5)$$

where $t_1 - t_0 = t_2 - t_1 = \dots = t_j - t_{j-1} = \Delta t$ (sampling period).

Note that, in (4) and (5) the upper switch (S_x) (where $x = 1, 2, \dots, 2n$) is the main responsible switch for charging and discharging the SM's capacitor. It also worth noting that due to the small internal resistance of the semiconductor switch, the voltage drop caused by S_x is neglected in this analysis. Furthermore, knowledge of the switching states obtained directly from the processor without including the voltage drop has been proven to be sufficient for estimation methods [26, 27, 29]. However, while this drop is described as negligible in [26, 27, 29], the actual values are not indicated. Nevertheless, it is easy to estimate this drop in order to improve the accuracy of the proposed model. Section V illustrates more details on the effect of such a voltage drop on the system model.

A. Proposed Voltage Estimation Technique

In general, the ERLS algorithm has two main advantages over the normal mean least square (MLS) and the conventional recursive least square (RLS) algorithms [30, 31]. 1) The computation time is reduced, which is very important for the real time implementation, and 2) it has the ability to cope with time-varying dynamic systems. Therefore, it can be suitable for power converter systems where parameter and state estimators can be used to reduce system complexity and cost.

The ERLS algorithm has been well-detailed in [30, 31], however, for the benefit of the reader, it is simplified here again. Assume that a real dynamic system can be described as follows:

$$\mathbf{y}(t_i) = z_1(t_i)\boldsymbol{\theta}_1(t_i) + z_2(t_i)\boldsymbol{\theta}_2(t_i) + \dots + z_n(t_i)\boldsymbol{\theta}_n(t_i) \quad (6)$$

Where the target is to find the estimated values of $\boldsymbol{\theta}_1(t_i), \boldsymbol{\theta}_2(t_i), \dots, \boldsymbol{\theta}_n(t_i)$ in which $i = 1, 2, 3, \dots, j$, $\mathbf{y}(t_i)$ is the available measured data, and $z_1(t_i), z_2(t_i), \dots, z_n(t_i)$ are also accessible and known data. In a matrix form, (6) can be rewrite in a linear regression as follows:

$$\mathbf{y}(t_i) = \mathbf{z}^T(t_i)\boldsymbol{\theta}(t_i) \quad (7)$$

The implementation sequence of the ERLS algorithm on the model described above for finding $\boldsymbol{\theta}$ values is demonstrated in Table II [30, 31]. It is important to indicate that in order to achieve accurate estimation of the $\hat{\boldsymbol{\theta}}$, the weighted sum of the quadratic error (i.e. cost function) is calculated as follows [32]:

$$J_u = \sum_{i=1}^j \lambda^{j-i} (\mathbf{y}(t_i) - \mathbf{z}^T(t_i)\hat{\boldsymbol{\theta}}(t_i))^2 \quad (8)$$

where λ is known as a forgetting factor. The smaller the forgetting factor is, the faster tracking of time-varying unknown parameter will be, however the algorithm will be more sensitive to noise. Therefore, a care has to be

taken when λ is chosen, each system has its own preference. However, it is recommended that this factor should be chosen within the range of: $0 << \lambda < 1$ [30].

Table. II ERLS adaptive algorithm

Step	Action and related equation
1. Initialisation	Initiate $P(t_0)$, $\hat{\boldsymbol{\theta}}(t_0)$ and λ
2. Calculate the gain	$K(t_i) = \frac{P(t_{i-1})z(t_i)}{(z^T(t_i)P(t_{i-1})z(t_i) + \lambda)}$
3. Calculate prediction error	$e_{y(t_i)} = \mathbf{y}(t_i) - \hat{\mathbf{y}}(t_i)$, $\hat{\mathbf{y}}(t_i) = \mathbf{z}^T(t_i)\hat{\boldsymbol{\theta}}(t_i)$
4. Update the parameter $\hat{\boldsymbol{\theta}}$	$\hat{\boldsymbol{\theta}}(t_i) = \hat{\boldsymbol{\theta}}(t_{i-1}) + K(t_i)e_{y(t_i)}$
5. Update the covariance matrix P	$P(t_i) = \frac{1}{\lambda} [(P(t_{i-1})) - (K(t_i)z^T(t_i)P(t_{i-1}))]$

It is found that, by employing this algorithm to the MMC model described by (4) and (5), the estimation of the individual SM capacitors' voltage can be accomplished. The arm voltage model of the upper and lower arm in (4) and (5) can be rewritten as follows:

$$\mathbf{u}_u(t_i) = [S_x^T(t_i)][\mathbf{V}_{cx}(t_i)] \quad (9)$$

$$\mathbf{u}_l(t_i) = [S_x^T(t_i)][\mathbf{V}_{cx}(t_i)] \quad (10)$$

Note that, in equation (9) $x = 1, 2, \dots, n$ and in equation (10) $x = (n + 1), (n + 2), \dots, 2n$.

where $i = 1, 2, 3, \dots, j$, note that similar to (7), equations (9) and (10) are also linear. Similarity in these equations (i.e. (7), (9) and (10)) allows applying the ERLS algorithm to the MMC easily. The only difference is to substitute $\mathbf{y}(t_i), z(t_i)$ and $\boldsymbol{\theta}(t_i)$ in (7) by the total SM arm voltage $\mathbf{u}_u(t_i)$ or $\mathbf{u}_l(t_i)$, switching states $S_x(t_i)$ and SM voltage $\mathbf{V}_{cx}(t_i)$.

Since the ERLS algorithm is applied to the upper and lower arms independently, only upper arm is described in this section.

To initiate the ERLS estimation algorithm as illustrated in Table II, $P(t_i)$ (covariance matrix), λ and $\hat{\mathbf{V}}_{cx}(t_i)$ (estimated SM voltage) must be specified with initial values of $P(t_0)$, 0.851 and $\hat{\mathbf{V}}_{cx}(t_0)$ respectively, in which:

$$P(t_0) = GI \quad (11)$$

In (11), G is a constant positive number, (and it is preferable for G to be a large number [30]). In this implementation $G = 1 \times 10^3$ and I is $n \times n$ identical matrix, where n is the number of the SMs within the upper arm, whilst $\hat{\mathbf{V}}_{cx}(t_0)$ is assumed to be zero (i.e. the capacitors considered initially uncharged).

After defining $P(t_0)$ and $\hat{\mathbf{V}}_{cx}(t_0)$, an adaptive gain $K(t_i)$ is calculated based on the sequence implementation shown in Table II as:

$$K(t_i) = \frac{P(t_{i-1}) S_x(t_i)}{(S_x^T(t_i) P(t_{i-1}) S_x(t_i) + \lambda)} \quad (12)$$

The main idea of the proposed estimation algorithm is to minimise the error between the total measured arm SMs voltages ($\mathbf{u}_u(t_i)$) and their estimated values ($\hat{\mathbf{u}}_u(t_i)$):

$$e_{\mathbf{u}(t_i)} = \mathbf{u}_u(t_i) - \hat{\mathbf{u}}_u(t_i) \quad (13)$$

where $e_{\mathbf{u}(t_i)}$ is the prediction error for the total voltage SMs of upper arm. The cost function for total voltage arm which identify the weighted sum of the quadratic error is given by:

$$J_u = \sum_{i=1}^j \lambda^{j-i} (\mathbf{u}_u(t_i) - \hat{\mathbf{u}}_u(t_i))^2 \quad (14)$$

To estimate the voltage value in one prediction step ahead, the previous voltage at t_{i-1} ($\hat{\mathbf{V}}_{cx}(t_{i-1})$) has to be included in the algorithm process as well as the error calculated in (13) multiplied by the adaptive gain ($K(t_i)$) which has been calculated in (12). In the first initial step $\hat{\mathbf{V}}_{cx}(t_0) = \hat{\mathbf{V}}_{cx}(t_i - 1) = 0$, therefore, achieving this goal for the estimation of the upper capacitor voltages at t_i is achieved as follows:

$$\hat{\mathbf{V}}_{cx}(t_i) = \hat{\mathbf{V}}_{cx}(t_i - 1) + K(t_i) e_{\mathbf{u}(t_i)} \quad (15)$$

The new covariance matrix ($P(t_i)$) is then updated with $K(t_i)$ as follows:

$$P(t_i) = \left(\frac{1}{\lambda} \right) \left[P(t_i - 1) - \left(\frac{P(t_{i-1}) S_x(t_i) S_x^T(t_i) P(t_{i-1})}{(\lambda + S_x^T(t_i) P(t_{i-1}) S_x(t_i))} \right) \right] \quad (16)$$

For simplicity, the proposed algorithm is summarised in the following flowchart (Fig.3):

The block diagram of the proposed estimation topology, including the voltage-balancing algorithm for the upper arm is shown in Fig. 4. For the lower arm of the converter, the same algorithms are processed. However, some rearrangements have to be considered. For example, in (12), (15) and (16) $x = n + 1, n + 2 \dots 2n$ instead of $x = 1, 2 \dots n$. It worth noting that the sorting algorithm used in Fig. 4 is similar to that presented in [12], and it should be also noted that, the voltage-balancing (i.e. the sorting algorithm) used in this paper has nothing to do with the proposed estimation method. However, in the present research, achieving voltage-balancing relies on estimated voltages of the SM capacitors rather than their measured values. Therefore, sorting these voltages ($\hat{\mathbf{V}}_{c1} \sim \hat{\mathbf{V}}_{cn}$ and $\hat{\mathbf{V}}_{c(n+1)} \sim \hat{\mathbf{V}}_{c2n}$) is evaluated in descending order to charge and discharge the most desired capacitors; where the states of the capacitors (charging and discharging) depend on arm current direction.

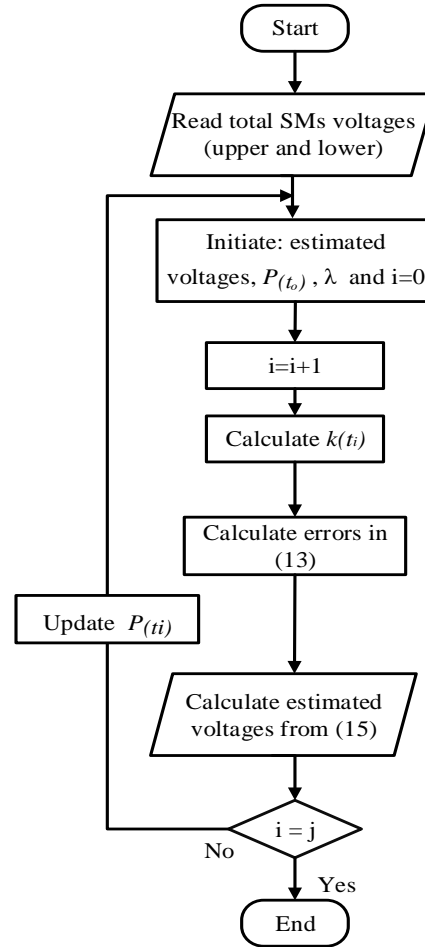


Fig.3. Flow chart of the proposed SMs voltages estimation method for the upper arm.

Therefore, monitoring the arm current is mandatory. Furthermore, phase disposition sinusoidal pulse-width modulation (PD-PWM) strategy is used, where r carrier signals with the same phase and different levels are required for N -level.

The voltage-balancing method used for the upper arm is shown in Fig. 5, where more detail about the technique can be found in [12].

As a result, PWM_n and $PWM_{\bar{n}}$ will be applied to the converter with a unit delay (Z^{-1}) in order to switch S_n and \bar{S}_n , respectively in the appropriate time. A dead-time period is added to $PWM_{\bar{n}}$ before switching \bar{S}_n . In consequence of a very small voltage drop caused when S_n and \bar{S}_n are activated, it is assumed that $PWM_n = S_n$ and $PWM_{\bar{n}} = \bar{S}_n$.

I. SIMULATION STUDIES

In order to verify the proposed estimation technique for the MMC, a single-phase 9-level MMC is considered and simulated using MATLAB software package. Eight SMs per arm ($x = 16$) are used to construct this converter and only one voltage sensor for each arm is used. The system parameters are tabulated in Table III. The effectiveness of the proposed

technique is confirmed through different experiments as discussed in the following cases.

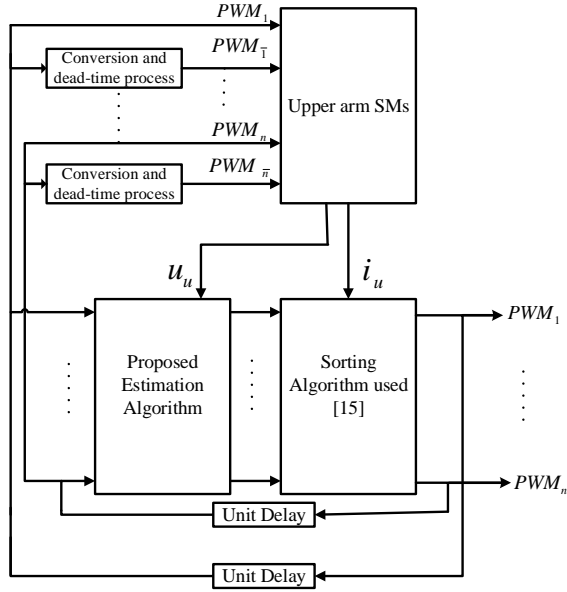


Fig.4. The proposed estimation method and the associated sorting algorithms for the upper arm control.

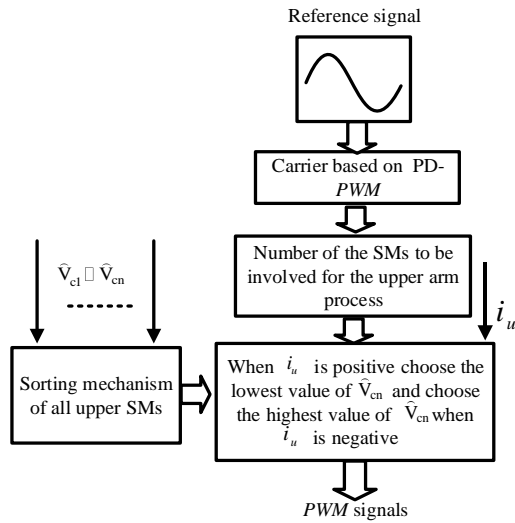


Fig. 5. Block diagram of the upper arm voltage-balancing strategy used.

A. Case I: the performance of the proposed method for the normal operating condition

In this case the performance of the 9-level MMC is evaluated under normal steady-state operating conditions, where the converter is assumed to work with a constant R-L load. Voltage sensors are used for each SM at first to measure the capacitor voltages as shown in Fig. 6 (a)-(c). The performance of the converter with the proposed method is illustrated in Fig. 7 (a)-(c). Owing to a small error between the measured and estimated voltages, voltages across the upper and lower arm capacitors in Fig. 7 (a) show extra deviation compared to those presented in Fig. 6 (a). However, this small difference between the signals in Figs 6(a) and

7(a) does not have any notable effect on the converter output voltage and current as can be clearly seen from Fig. 7 (b), and (c). This confirms the accuracy of the proposed technique. Moreover, it should also be noted that the sensor-based measurement technique requires 16 voltage sensors for the 9-level MMC, while the proposed estimation technique needs only two voltage sensors to achieve voltage-balancing of the converter.

TABLE III
PARAMETERS OF THE SIMULATED 9-LEVEL SINGLE-PHASE MMC

Parameter	Value
SM capacitor (C)	3800 μ F
Modulation index (m_t)	0.80
DC-link voltage (V_{dc})	10 kV
Output frequency (f)	50 Hz
Carrier switching frequency (f_s)	2.5 kHz
Number of SM per leg (N)	16
Load resistor (R)	33 Ω
Arm inductor (L_S)	4.4 mH
Load inductor (L)	15 mH
Sampling frequency ($f_{sampling}$)	20 kHz

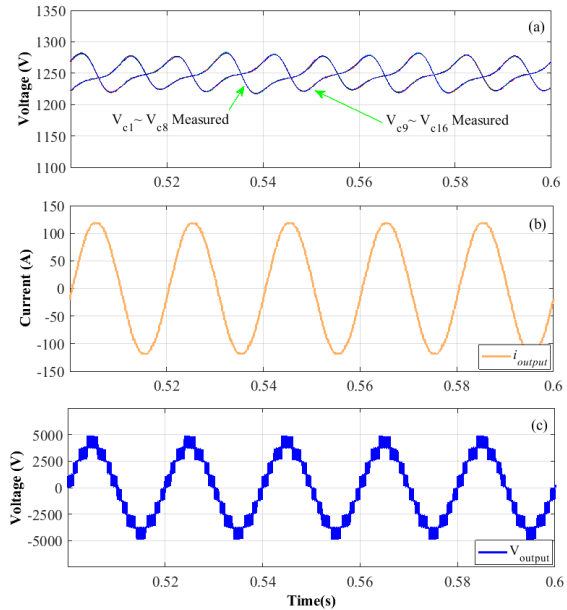


Fig.6. Simulation results of the 9-level MMC with the sensor-based measuring technique. (a) Upper and lower capacitor voltages $V_{c1} \sim V_{c8}$ & $V_{c9} \sim V_{c16}$. (b) Output current. (c) Output voltage.

B. Case II: performance of the proposed method with capacitance deviation

To further validate the effectiveness of the proposed scheme, deviations in SMs capacitance is considered in this case.

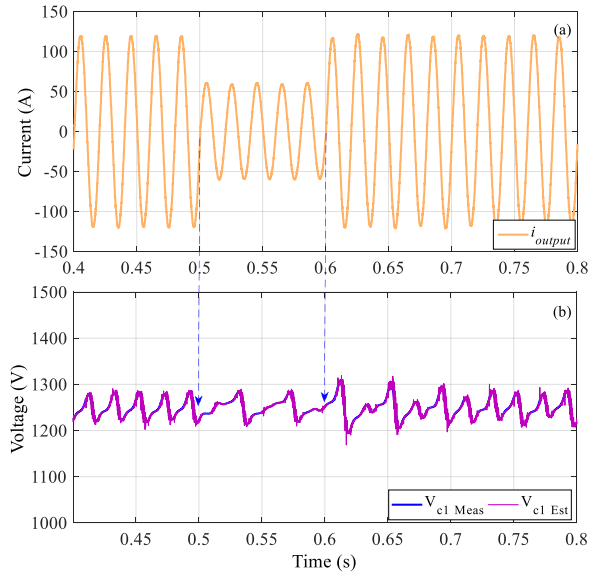


Fig.10. Simulation results for the 9-level MMC with step load change. (a) Output current. (b) Upper arm capacitor voltages across C_1 .

D. Case IV: Start-up performance.

In this part of the simulation study, start-up performance is reported in Fig. 11. It is clear that from the figure the proposed ERLS algorithm tracks the measured voltage very quickly.

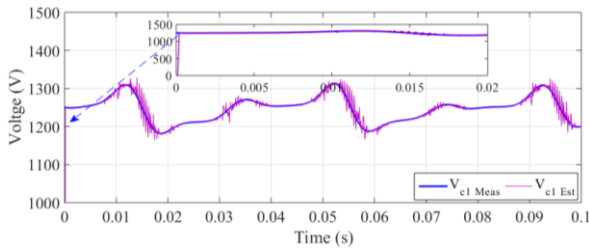


Fig. 11. Start-up transient condition performance of the proposed estimation method.

E. Case V: The performance of the proposed method during DC voltage change.

An extreme change is applied to the system to further validate the method where the DC voltage of the converter is suddenly dropped. Fig. 12 (a) and (b) show the corresponding changes in the output current and voltage when the estimation method is used. In addition, Fig 12 (c) shows the measured and the estimated voltage across C_1 . It is obvious that the estimated voltage can successfully track this extreme change.

Another sudden change in the DC voltage is applied in Fig. 13, where the DC voltage is increased this time by around 90%. Similar to the previous case where the DC voltage dropped, the estimated voltage across C_1 successfully tracks the measured voltage.

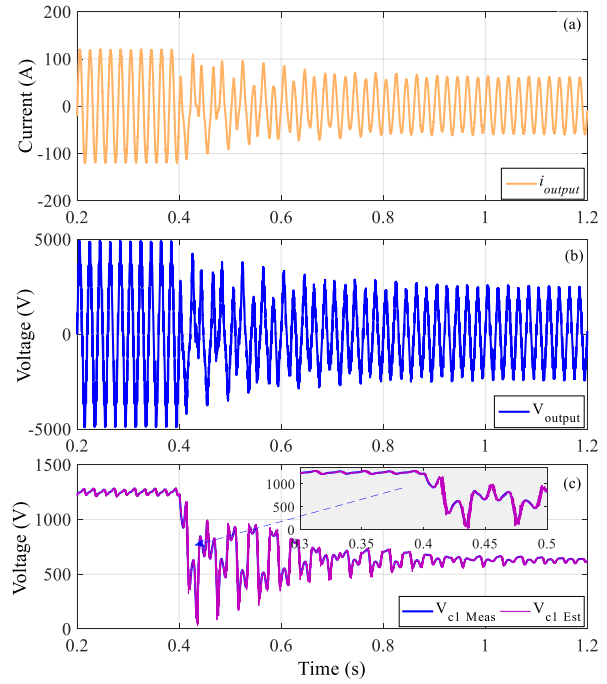


Fig. 12. The performance of the proposed method during DC voltage change. (a) The output current response. (b) The output voltage response. (c) Measured and estimated voltage across C_1 .

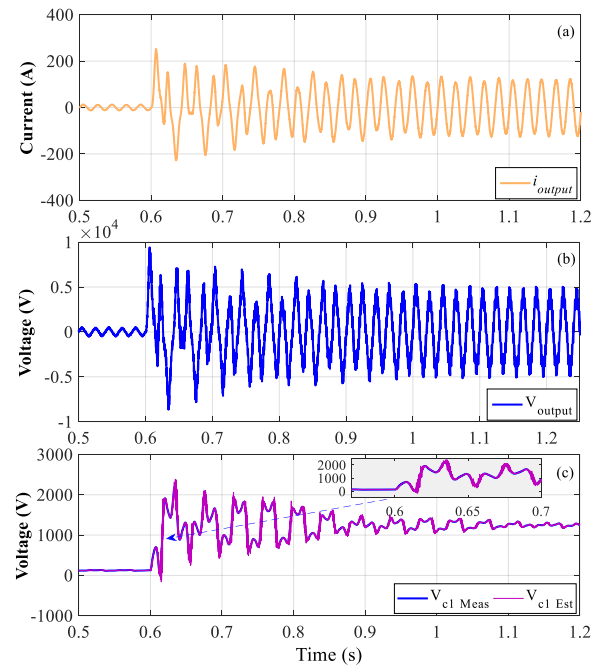


Fig. 13. The performance of the proposed method during sudden increase in the DC voltage. (a) The output current response. (b) The output voltage response. (c) Measured and estimated voltage across C_1 .

V. EXPERIMENTAL STUDIES

To practically evaluate and validate the proposed method, a scaled-down system for a single-phase 4-level MMC laboratory prototype has been built. Fig. 14 illustrates the experimental setup for the system. A photograph of the experimental test bench is illustrated in Fig. 15. Three SMs per arm are placed ($n=3$) with an R-L load, where an IRF530N power MOSFET is used to construct the converter. The half-bridge SM

capacitor is the VISHAY 56 1000 μ F 63 V DC with $\pm 20\%$ tolerance. The converter is fed with an EX354RT TRIPLE 300W power supply. Other details of the converter parameters are summarized in Table IV.

To control the converter, a TMS320F28335 floating point microcontroller is used. The proposed algorithm and the voltage-balancing algorithm are uploaded to the controller with the help of Code Composer Studio (CCS5.5) development tools. The execution time of the proposed estimation method for the upper and lower arm as well as the voltage-balancing algorithm is approximately 34 μ s. The carrier frequency of the MMC is 2.5 kHz while the dead-time (as demonstrated in Fig. 4) between the upper and lower switches of the same SM is 3 μ s. Three CAS-15 current sensors are used to monitor the upper, lower arm and output current of the converter while six LV25-P voltage sensors are used to compare the real and the estimated capacitor voltages. For the arm voltage measurement, two AD215AY isolation amplifier sensors are used.

TABLE IV
EXPERIMENTAL PARAMETERS

Parameter	Value
SM capacitor (C)	1000 μ F
Modulation index (m_i)	0.9
DC-link voltage (V_{dc})	60V
Output frequency (f)	50 Hz
Carrier frequency (f_c)	2.5 kHz
Number of SM per leg (N)	6
Load resistor (R)	33 Ω
Arm inductor (L_s)	1 mH
Load inductor (L)	4 mH
Sampling frequency ($f_{sampling}$)	20 kHz

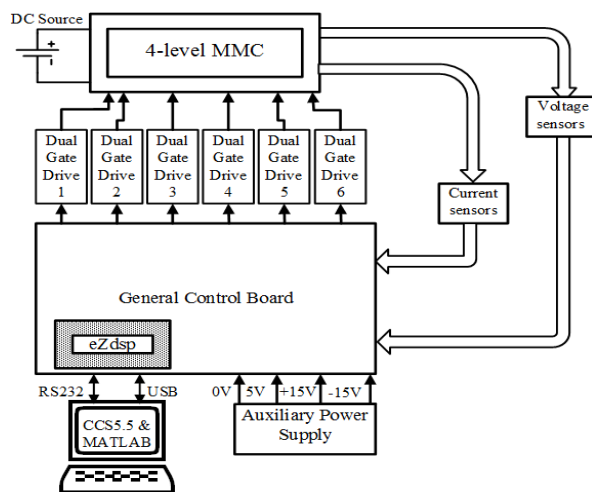


Fig. 14. Block diagram of the experimental set-up.

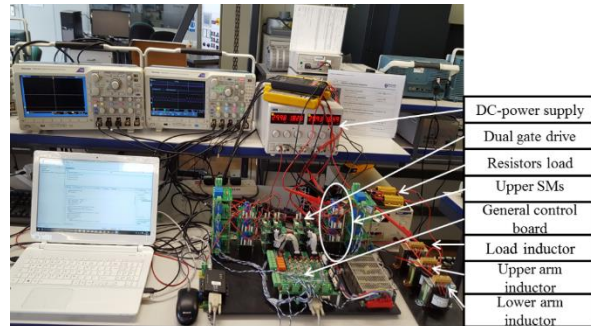


Fig. 15. A photograph of the experimental test bench.

An intensive testing and experiments are conducted to validate the simulation and the theoretical studies. Realistically there will always be some deviations between ideal and practical systems caused by various factors. The voltage drop due to the internal resistance of the semiconductor devices ($S_x drop$) and the stray impedance of the connecting wires ($V_{Line x drop}$) are two examples. However, stray inductance is neglected in this analysis. To experimentally validate the assumption made earlier that it has a minimal effect on the performance of the proposed method and can be ignored; equation (4) is experimentally implemented as example and the result is shown in Fig. 16. This was accomplished using External MATLAB mode, where the data inside the DSP (TMS320F28335) can be accessed in real-time processing. As it can be clearly seen from Fig. 16, there is a very small difference between the two signals (blue and red), which is caused by the practical aspects explained above. This therefore confirms the assumption and these voltage drops can be safely neglected in the calculation without having a significant impact on the system model. However, for a more accurate formula of the four-level MMC, equation (4) can be rewritten as follows:

$$\mathbf{u}_u = S_1 * \mathbf{V}_{c1} + S_1 drop + V_{Line 1 drop} + \dots + S_3 * \mathbf{V}_{c3} + S_3 drop + V_{Line 3 drop} \quad (17)$$

It should be noted that a similar equation can be written for \mathbf{u}_l , Fig. 17 illustrates \mathbf{u}_u in comparison with the total lower arm voltage \mathbf{u}_l and the output voltage \mathbf{u}_a .

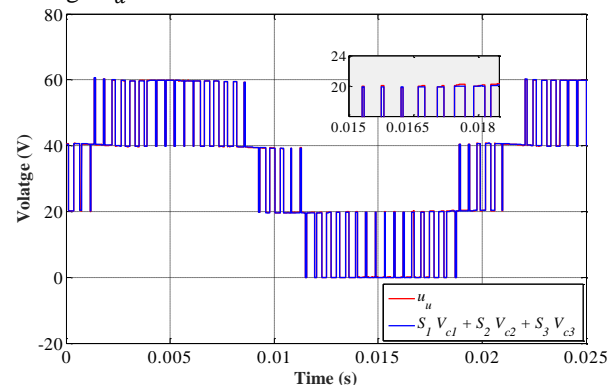


Fig.16. Experimental results for measured (\mathbf{u}_u) and calculated ($S_1 \mathbf{V}_{c1} + S_2 \mathbf{V}_{c2} + S_3 \mathbf{V}_{c3}$) total upper arm voltage.

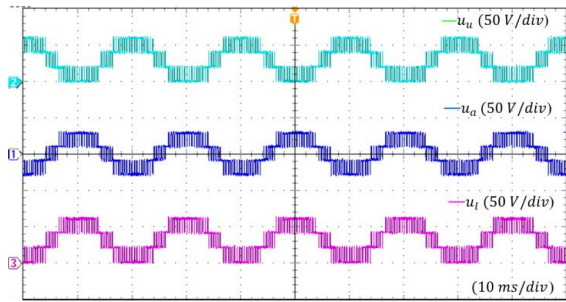


Fig.17. Total upper arm voltage u_u , output voltage u_a and lower arm voltage u_l .

Experimental results of the sensor-based measurement and the proposed technique based on steady-state condition are presented in Figs. 18 and 19. Figs. 18 (a) and 19 (a) show the three upper SM capacitor voltages, $V_{c1} \sim V_{c3}$. It can be observed that Fig 19 (a) shows a slight deviation in comparison with Fig. 18 (a). However, this does not have a notable impact neither on the output current nor on the output voltage as illustrated in Fig.-19 (b). Interestingly, zoomed-in samples of Fig 18 and 19 verify this; however, only very small differences in the voltage waveforms can be observed as shown in Fig. 20, which is acceptable for the reduction in sensors count. Furthermore, with the proposed scheme, the same number of two sensors is sufficient to achieve voltage-balancing for even the N -level MMC. Additionally, comparison between the voltage across $C1$ achieved from the conventional sensor-based method and the proposed estimated method is illustrated in Fig. 21.

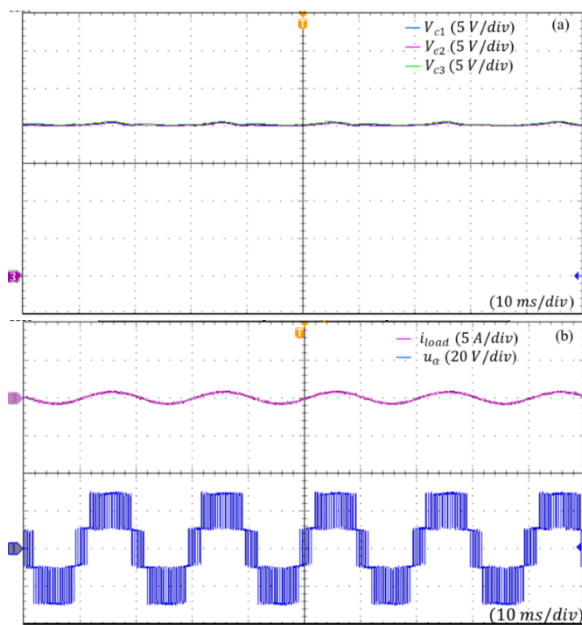


Fig. 18. Experimental results of the sensor-based measurement technique. (a) Three upper SM voltage capacitors. (b) Output current and voltage.

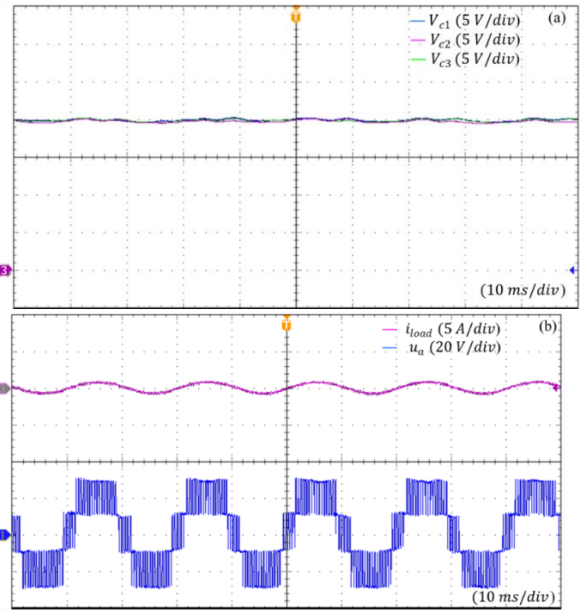


Fig. 19. Experimental results of the proposed estimation technique. (a) Three upper SM voltage capacitors. (b) Output current and voltage.

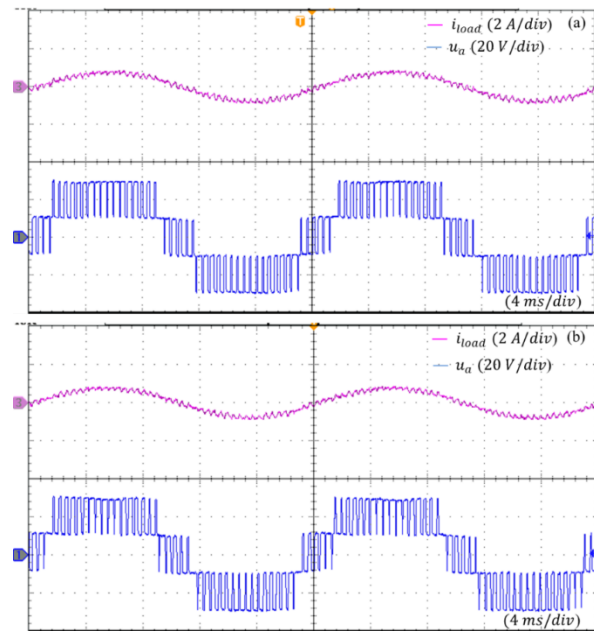


Fig. 20. Output current and voltage. (a) Results of the sensor-based measurement technique. (b) Results of the proposed estimation technique.

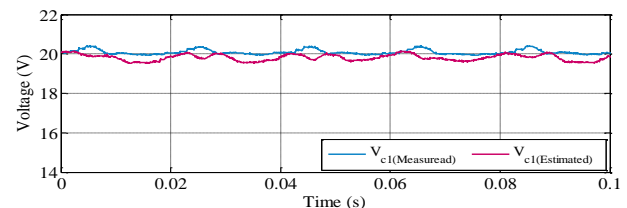


Fig. 21. Voltage comparison between the conventional sensor-based method and the proposed method across $C1$.

To further validate the robustness of the proposed technique for a step change in the load, additional experimental tests have been conducted by altering the load resistance (R). An additional resistance of $68\ \Omega$ is added and then removed from the load to stimulate the step change in the load. As it can be noted from Fig. 22, the converter was able to successfully achieve balancing.

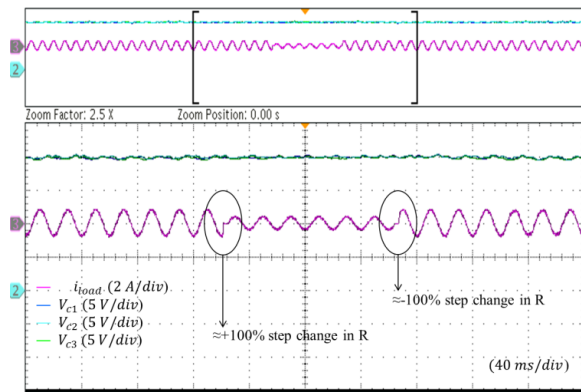


Fig. 22. Proposed scheme performance at step changes (increase and decrease) in R .

Other dynamic operation analyses have been conducted to verify the proposed method in the case of DC voltage change occurs and when a sudden extreme change in the DC voltage is applied to the converter. Fig. 23 illustrates the DC voltage change emulation when the input volt has been decreased by $\approx 90\%$. It can be observed that the \hat{V}_{c1} can successfully follow up this change to reach its reference value ($\frac{V_{dc}}{n}$). An extra extreme change is also investigated in Fig. 24; where about 90% increase in the DC voltage is applied to the converter. The proposed method quickly and successfully responds to this change, which confirms the simulation results.

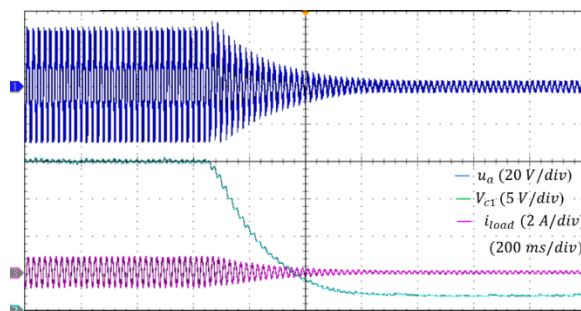


Fig. 23. Extreme change occurs in the DC voltage and the corresponding changes in the \hat{V}_{c1} , output voltage and current.

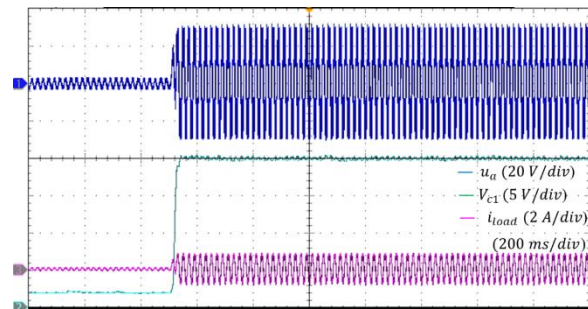


Fig. 24. Extreme increase in the DC voltage value and the corresponding changes in the \hat{V}_{c1} , output voltage and current.

V. CONCLUSION

In this paper, a new measurement estimation technique for MMC is proposed in which a novel SM voltage estimation scheme is developed using the ERLS algorithm. Detailed simulation and experimental tests for a single-phase MMC were conducted to demonstrate the effectiveness of the proposed scheme in steady-state and dynamic operating conditions. Various tests have been carried out for the converter to investigate the effect of capacitance deviations, sudden change in load conditions, DC voltage change and start-up transient condition. Results confirmed the capability of the proposed method to provide accurate voltage estimation and achieve the capacitor voltage-balancing of the converter with only one voltage sensor per arm. The effect of voltage drops in the SM switch and wire resistance between SMs on the proposed model has been also evaluated. With this proposed technique, any voltage-balancing method can be used. This improvement allows a significant reduction in the number of voltage sensors required. As a result, this improvement will reduce the total cost and the complexity of the converter. Application of this technique will also improve system reliability, especially when the MMC reaches high output levels. Finally, the proposed method can be equally applied to the FCC and CHC.

REFERENCES

- [1] A. Lesnicar and R. Marquardt, "An Innovative Modular Multilevel Converter Topology Suitable for a Wide Power Range," in *Power Tech Conference Proceedings, 2003 IEEE Bologna*, 2003, p. 6 pp. Vol.3.
- [2] S. Debnath, J. Qin, B. Bahrani, M. Saefidard, and P. Barbosa, "Operation, Control, and Applications of the Modular Multilevel Converter: A Review," *IEEE Transactions on Power Electronics*, vol. 30, pp. 37-53, 2015.
- [3] M. Guan and Z. Xu, "Modeling and Control of a Modular Multilevel Converter-Based HVDC System Under Unbalanced Grid Conditions," *IEEE Transactions on Power Electronics*, vol. 27, pp. 4858-4867, 2012.
- [4] M. A. Perez, S. Bernet, J. Rodriguez, S. Kouro, and R. Lizana, "Circuit Topologies, Modeling, Control Schemes, and Applications of Modular Multilevel Converters," *IEEE Transactions on Power Electronics*, vol. 30, pp. 4-17, 2015.
- [5] M. Glinka and R. Marquardt, "A new AC/AC multilevel converter family," *IEEE Transactions on Industrial Electronics*, vol. 52, pp. 662-669, 2005.

- [6] M. A. Parker, L. Ran, and S. J. Finney, "Distributed Control of a Fault-Tolerant Modular Multilevel Inverter for Direct-Drive Wind Turbine Grid Interfacing," *IEEE Transactions on Industrial Electronics*, vol. 60, pp. 509-522, 2013.
- [7] K. Ou, H. Rao, Z. Cai, H. Guo, X. Lin, L. Guan, et al., "MMC-HVDC Simulation and Testing Based on Real-Time Digital Simulator and Physical Control System," *IEEE Journal of Emerging and Selected Topics in Power Electronics*, vol. 2, pp. 1109-1116, 2014.
- [8] J. Lyu, X. Cai, and M. Molinas, "Frequency Domain Stability Analysis of MMC-Based HVdc for Wind Farm Integration," *IEEE Journal of Emerging and Selected Topics in Power Electronics*, vol. 4, pp. 141-151, 2016.
- [9] H. Akagi, "Classification, Terminology, and Application of the Modular Multilevel Cascade Converter (MMCC)," *IEEE Transactions on Power Electronics*, vol. 26, pp. 3119-3130, 2011.
- [10] G. Bergna, E. Berne, P. Egrot, P. Lefranc, A. Arzande, J. C. Vannier, et al., "An Energy-Based Controller for HVDC Modular Multilevel Converter in Decoupled Double Synchronous Reference Frame for Voltage Oscillation Reduction," *IEEE Transactions on Industrial Electronics*, vol. 60, pp. 2360-2371, 2013.
- [11] G. Konstantinou, J. Pou, S. Ceballos, R. Picas, J. Zaragoza, and V. G. Agelidis, "Control of Circulating Currents in Modular Multilevel Converters through Redundant Voltage Levels," *IEEE Transactions on Power Electronics*, vol. PP, pp. 1-1, 2016.
- [12] S. Li, X. Wang, Z. Yao, T. Li, and Z. Peng, "Circulating Current Suppressing Strategy for MMC-HVDC Based on Nonideal Proportional Resonant Controllers Under Unbalanced Grid Conditions," *IEEE Transactions on Power Electronics*, vol. 30, pp. 387-397, 2015.
- [13] C. Oates, "Modular Multilevel Converter Design for VSC HVDC Applications," *IEEE Journal of Emerging and Selected Topics in Power Electronics*, vol. 3, pp. 505-515, 2015.
- [14] F. Deng, Z. Chen, M. R. Khan, and R. Zhu, "Fault Detection and Localization Method for Modular Multilevel Converters," *IEEE Transactions on Power Electronics*, vol. 30, pp. 2721-2732, 2015.
- [15] M. Saeedifard and R. Iravani, "Dynamic Performance of a Modular Multilevel Back-to-Back HVDC System," *IEEE Transactions on Power Delivery*, vol. 25, pp. 2903-2912, 2010.
- [16] M. Hagiwara and H. Akagi, "Control and Experiment of Pulsewidth-Modulated Modular Multilevel Converters," *IEEE Transactions on Power Electronics*, vol. 24, pp. 1737-1746, 2009.
- [17] S. Fan, K. Zhang, J. Xiong, and Y. Xue, "An Improved Control System for Modular Multilevel Converters with New Modulation Strategy and Voltage Balancing Control," *IEEE Transactions on Power Electronics*, vol. 30, pp. 358-371, 2015.
- [18] P. M. Meshram and V. B. Borghate, "A Simplified Nearest Level Control (NLC) Voltage Balancing Method for Modular Multilevel Converter (MMC)," *IEEE Transactions on Power Electronics*, vol. 30, pp. 450-462, 2015.
- [19] A. Dekka, B. Wu, N. R. Zargari, and R. L. Fuentes, "Dynamic Voltage Balancing Algorithm for Modular Multilevel Converter: A Unique Solution," *IEEE Transactions on Power Electronics*, vol. 31, pp. 952-963, 2016.
- [20] J. Zhang, Z. Wang, and S. Shao, "A Three-Phase Modular Multilevel DC-DC Converter for Power Electronic Transformer Applications," *IEEE Journal of Emerging and Selected Topics in Power Electronics*, vol. 5, pp. 140-150, 2017.
- [21] T. Soong and P. W. Lehn, "Internal Power Flow of a Modular Multilevel Converter With Distributed Energy Resources," *IEEE Journal of Emerging and Selected Topics in Power Electronics*, vol. 2, pp. 1127-1138, 2014.
- [22] A. Dekka, B. Wu, N. R. Zargari, and R. L. Fuentes, "A Space-Vector PWM-Based Voltage-Balancing Approach With Reduced Current Sensors for Modular Multilevel Converter," *IEEE Transactions on Industrial Electronics*, vol. 63, pp. 2734-2745, 2016.
- [23] F. Deng and Z. Chen, "Voltage-Balancing Method for Modular Multilevel Converters Switched at Grid Frequency," *IEEE Transactions on Industrial Electronics*, vol. 62, pp. 2835-2847, 2015.
- [24] F. Deng and Z. Chen, "A Control Method for Voltage Balancing in Modular Multilevel Converters," *IEEE Transactions on Power Electronics*, vol. 29, pp. 66-76, 2014.
- [25] K. Ilves, A. Antonopoulos, S. Norrga, and H. P. Nee, "A New Modulation Method for the Modular Multilevel Converter Allowing Fundamental Switching Frequency," *IEEE Transactions on Power Electronics*, vol. 27, pp. 3482-3494, 2012.
- [26] S. Shao, P. W. Wheeler, J. C. Clare, and A. J. Watson, "Fault Detection for Modular Multilevel Converters Based on Sliding Mode Observer," *IEEE Transactions on Power Electronics*, vol. 28, pp. 4867-4872, 2013.
- [27] H. Nademi, A. Das, and L. E. Norum, "Modular Multilevel Converter With an Adaptive Observer of Capacitor Voltages," *IEEE Transactions on Power Electronics*, vol. 30, pp. 235-248, 2015.
- [28] G. S. Silva, R. P. Vieira, and C. Rech, "Discrete-Time Sliding-Mode Observer for Capacitor Voltage Control in Modular Multilevel Converters," *IEEE Transactions on Industrial Electronics*, vol. PP, pp. 1-1, 2017.
- [29] R. Picas, J. Zaragoza, J. Pou, S. Ceballos, and J. Balcells, "New Measuring Technique for Reducing the Number of Voltage Sensors in Modular Multilevel Converters," *IEEE Transactions on Power Electronics*, vol. 31, pp. 177-187, 2016.
- [30] J. A. Apolinário and J. G. McWhirter, *QRD-RLS Adaptive Filtering*: Brazil, Springer, 2009.
- [31] S. S. Haykin, *Adaptive filter theory*: Pearson Education India, 2008.
- [32] A. Vahidi, A. Stefanopoulou, and H. Peng, "Recursive least squares with forgetting for online estimation of vehicle mass and road grade: theory and experiments," *Vehicle System Dynamics*, vol. 43, pp. 31-55, 2005.



Osama SH Mohamed Abushafa

received the B.Sc. degree in Electrical and Electronic Department from Sirt University, Albregah, Libya in 2001, M.Sc. and the Ph.D. degrees from Newcastle University, Newcastle upon Tyne, U.K., in 2010, and 2017. From 2010 to 2012, he was an Assistant Lecturer with the Department of Electrical and Electronic Department, Zawia University. In 2013, he joined the Electrical Power Research Group, Newcastle University, as a PhD researcher in Power Electronics. Since November 2017, Dr Osama has joined Turbo Power Systems LTD company. Dr. Osama has been recently a Regular Reviewer for IEEE journals



Shady Gadoue

received the B.Sc. and M.Sc. degrees from Alexandria University, Alexandria, Egypt, in 2000 and 2003, respectively, and the Ph.D. degree from Newcastle University, Newcastle upon Tyne, U.K., in 2009, all in Electrical Engineering. From 2009 to 2011, he was an Assistant Professor with the Department of Electrical Power Engineering, Alexandria University. In 2011, he joined the Electrical Power Research Group, Newcastle University, as a Lecturer in Control Systems. Since March 2016, Dr Gadoue

has been a visiting member of academic staff with the Control and Power Research Group at Imperial College London, U.K. In Aug 2017, he joined the School of Engineering and Applied Science, Aston University, Birmingham as a Senior Lecturer. His main research interests include control, state and parameter identification, and optimization algorithms applied to energy conversion and power electronic systems.



Mohamed S. A. Dahidah (M'02–SM'10) received the Ph.D. degree in electrical engineering from Multimedia University, Malaysia, in 2008. In November 2007, he was appointed an Assistant Professor in the Department of Electrical and Electronic Engineering, The University of Nottingham, Malaysia Campus. He is currently with the School of Engineering, Newcastle University, Newcastle Upon Tyne, U.K. He has authored or co-authored a number of refereed journal and conference papers. His research interests include modular multilevel converters, SHE-PWM modulation technique for power electronics converters, battery charger for EVs, solid state transformers and renewable energy integration.

Dr. Dahidah is the Deputy Editor-in-Chief for *IET Power Electronics* and has been a Regular Reviewer for both IEEE and IET journals.



David J. Atkinson obtained his BSc in electrical and electronic engineering from Sunderland Polytechnic, England, in 1978 and his PhD from Newcastle University, England, in 1991. He is a Senior Lecturer in the Electrical Power Research Group at the School of Electrical and Electronic Engineering,

Newcastle University, UK. He joined the university in 1987 after 17 years in industry with NEI Reyrolle Ltd and British Gas Corporation. His research interests are focussed on the control of power electronics systems including electric drives and converters for renewable energy systems. Dr Atkinson is a chartered electrical engineer and a recipient of the Power Premium awarded by the Institution of Electrical Engineers (IEE).



Petros Missailidis received the B.S degree in mechanical engineering from Aristotelian University of Thessaloniki, Thessaloniki, Hellas, M.S. degree in mechanical engineering from the University of Buffalo, NY, USA, M.S. degrees in electrical, electronic engineering, biomedical engineering and Mathematics from Rensselaer Polytechnic Institute, Troy, NY, and the Ph.D. degree in mechanical engineering from Rensselaer Polytechnic Institute, in 2000. He was staff scientist with ComHouse Wireless Inc. Clemsford MA, senior electrical engineer M/A-COM Inc. Lowell MA, research associate at General Electric Schenectady NY and Erie County Medical Centre, Buffalo, NY, and post doctoral Fellow at the University of Toronto. He is currently with the School of Engineering, Newcastle University, Newcastle upon Tyne, UK. His interests are in the areas of System identification, Calculus of Variation and Optimal Control, Adaptive, Nonlinear control, Machine Learning, Number Theory, Electromagnetics